Multilevel Non-parametric Groupwise Registration in Cardiac MRI: Application to Explanted Porcine Hearts

Mia Mojica[1], Mihaela Pop[2], Maxime Sermesant[3], and Mehran Ebrahimi[1(✉)]

[1] Faculty of Science, University of Ontario Institute of Technology, Oshawa, ON, Canada
{mia.mojica,mehran.ebrahimi}@uoit.ca
[2] Department of Medical Biophysics, Sunnybrook Research Institute, University of Toronto, Toronto, ON, Canada
mihaela.pop@utoronto.ca
[3] Asclepios Team, INRIA, Sophia Antipolis, France
maxime.sermesant@inria.fr

Abstract. Statistical atlases of myocardial fiber directions have great utility in modelling applications. The first step in building atlases requires a registration of the hearts to a template. In this paper, we performed groupwise registration on a small database of explanted pig hearts ($N = 4$) and coupled it with a multilevel pairwise registration framework in order to generate an average cardiac geometry. The scheme implemented in our experiments effectively registers and normalizes the hearts despite a high variability in cardiac measurements. In addition, we adopted an intuitive averaging technique on the transformed versions of each heart to obtain a new reference geometry at every iteration. This reduces biases that may be introduced by the selection of an initial reference geometry in the construction of an average cardiac geometry. The next step will focus on improving current results by using a larger database of heart samples.

Keywords: Image registration · Inverse problems · Cardiac MRI
Multilevel registration · Non-parametric registration
Groupwise registration · Cardiac atlas

1 Introduction

Cardiovascular disease continues to be the leading cause of death, accounting for 30% of mortality worldwide [1]. There has been an increasing demand to understand the mechanical and electrical activities of the heart through the construction of atlases that model healthy hearts, against which pathological hearts can be compared. However, availability of explanted human hearts is scarce. Thus, studying large hearts (e.g. canine and pig hearts) could provide a good alternative as the cardiac anatomies and functions of the three species

M. Pop et al. (Eds.): STACOM 2017, LNCS 10663, pp. 60–69, 2018.
https://doi.org/10.1007/978-3-319-75541-0_7

are very similar. A statistical comparison between canine and human hearts in terms of their fiber orientations and their variability is provided in [2].

In this paper, we aim to lay the foundation of a framework for constructing a statistical atlas of a healthy porcine heart. To do this, we first need a registration framework that allows us to calculate transformations that would normalize their geometries. Specifically, we focus on the construction of an average cardiac geometry through groupwise registration of anatomical magnetic resonance (MR) images obtained using a diffusion-weighted method applied to a small database of porcine hearts (Fig. 1).

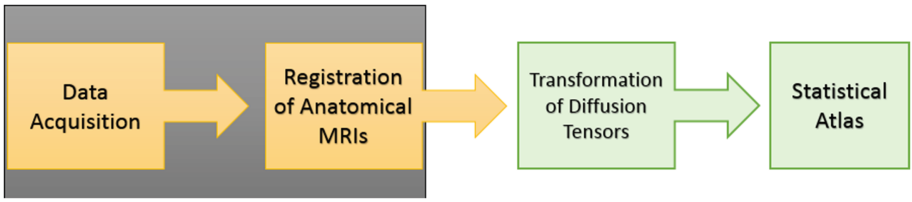

Fig. 1. Workflow diagram for building a statistical porcine cardiac atlas. Diffusion-weighted MR images of porcine hearts were acquired as discussed in Sect. 2.1, and then an average cardiac geometry was constructed through groupwise registration framework initialized by a multilevel affine and non-parametric pairwise registration scheme.

2 Methods

In this section, we discuss both the data acquisition methods and the registration framework used for our experiments.

2.1 Data Acquisition

All diffusion-weighted (DW) MRI studies were performed on a dedicated 1.5T GE Signa Excite scanner using freshly explanted healthy pig hearts [5]. In the current study, we used the following MR parameters: TE = 35 ms, TR = 700 ms, echo train length = 2, b-value = 0 for the unweighted MR images and $b = 500$ s/mm^2 when the seven diffusion gradients were applied, respectively. We used the same field of view (FOV) and a 256×256 k-space. The total scan time for DW imaging was approximately 8 h.

2.2 Pairwise Registration of the Anatomical MR Images

Constructing an average geometry for cardiac data is not trivial due to its variability in terms of scaling and spatial structures. Thus, we need to use an approach that caters to large deformations and assures the correct alignment of corresponding cardiac structures. In [2], a combination of constrained affine registration and hybrid intensity-based and feature-based non-rigid registration algorithm was used for the pairwise registration step. The constrained affine registration step

served to normalize the heights and radii of the hearts, while non-rigid registration ensured precise matching of cardiac structures. It is important to note, however, that the approach in [2] implied the need for selection of landmarks.

We followed the image registration outline proposed in [2] to align the hearts in the data set and come up with an average geometry. However, instead of using a non-rigid registration algorithm for pairwise registration, we used a combination of affine and non-parametric registration to align each subject to the current reference geometry. At every iteration, a reference geometry is obtained by computing the average of the transformations that register each of the hearts to the current reference geometry.

2.2.1 Mathematical Model

Given a template image $\mathcal{T} : \Omega \subset \mathbb{R}^3 \to \mathbb{R}$ and a reference image $\mathcal{R} : \Omega \subset \mathbb{R}^3 \to \mathbb{R}$, our goal is to find a reasonable transformation such that a transformed version of the template image $\mathcal{T}$ is similar to the reference $\mathcal{R}$ [10]. Mathematically, this can be modelled by solving the optimization problem

$$\min_{y} \mathcal{J}[y] = \mathcal{D}[\mathcal{T}[y], \mathcal{R}] + \mathcal{S}[y], \tag{1}$$

where $y : \Omega \to \mathbb{R}^3$ is the transformation that aligns $\mathcal{T}$ to $\mathcal{R}$, and $\mathcal{T}[y]$ is a transformed version of the template image $\mathcal{T}$.

The first term ($\mathcal{D}$) in the joint functional $\mathcal{J}$ measures the similarity between the two images and thus helps determine if there is a reasonable match between the image features. The second term ($\mathcal{S}$) is the regularization term, which makes the registration problem well-posed.

In our implementation, we used the sum of squared differences (SSD) for similarity measure, i.e.,

$$\mathcal{D}[\mathcal{T}[y], \mathcal{R}] = \frac{1}{2} \int_{\Omega} (\mathcal{T}[y](x) - \mathcal{R}(x))^2 \, dx. \tag{2}$$

The above integral is approximated using a midpoint quadrature rule on a cell-centered grid with mesh spacing h_i in each dimension $i \in \{1, 2, 3\}$. Its discretized form is given by

$$D^{\mathrm{SSD},h}(T^h, R^h) = \frac{1}{2} hd \|T^h - R^h\|^2,$$

with $hd = h_1 \cdot h_2 \cdot h_3$.

The regularization term $\mathcal{S}[y]$ enforces the functional to lead to a unique minimizer. In our experiments, we used the elastic potential of the transformation y for our regularization term [10]. It is given by

$$\mathcal{S}[y] = \text{Elastic Potential}[y - y^{\mathrm{ref}}].$$

2.2.2 Multilevel Representation of Data

In this paper, we used a multilevel registration scheme to initialize each iteration in the groupwise registration. With a multilevel approach, we start by solving

the minimization problem on a coarser level and then progress onto finer levels. The solutions on the coarser levels serve as starting guesses for the next (finer) levels. This is an efficient method for aligning two 3D images since computations on coarser levels are cheaper relative to those on finer levels. This approach also helps avoid running into local minimizers.

To obtain a smoothed measurement of an image in different levels, we get the average of the intensity values of adjacent cells. A detailed discussion on the computation of a multilevel representation of a 3D MR image can be found in [10].

2.2.3 Affine and Non-parametric Registration

From the coarsest to the finest level, we solve the discretized form of the optimization problem in (1), which is given by

$$\min_{y^h} \mathcal{J}^h \left[y^h\right] = \mathcal{D}\left(T^h, R^h; y^h\right) + \mathcal{S}\left(y^h - y^{\mathrm{ref},h}\right). \tag{3}$$

At the coarsest level, an affine parametric registration is performed. An affine transformation is one that preserves points, lines and planes. It allows for translation, rotation, scaling, and shearing.

An affine transformation $y = [y^1, y^2, y^3]^T$ of a point $[x^1, x^2, x^3]^T \in \mathbb{R}^3$ may be parametrized as

$$\begin{aligned} y^1 &= w_1 x^1 + w_2 x^2 \ + w_3 x^3 \ + w_4 \\ y^2 &= w_5 x^1 + w_6 x^2 \ + w_7 x^3 \ + w_8 \\ y^3 &= w_9 x^1 + w_{10} x^2 + w_{11} x^3 + w_{12}. \end{aligned}$$

The solution $y(w, x)$ to the affine registration problem [10] at the coarsest level will serve as the initial guess for the reference transformation y^{ref} for the elastic regularizer $\mathcal{S}[y]$ in the non-parametric registration step. That is, $y^{\mathrm{ref}} = y(w, x)$.

At every level, the minimization problem (3) is solved using a Gauss-Newton approach with an Armijo line search. The initial guess at every level is given by the prolongated version of the solution y^h from the preceding coarser level.

3 Groupwise Registration

Various methods have already been used to normalize cardiac geometries. In [4], a new reference geometry is computed each time an image in the data set is registered. Here, we adopted the method used in [8] and [2], where biases introduced by using one of the anatomical MR images as the first reference image were eliminated by registering the images to the same current reference geometry.

At every iteration, the reference geometry is updated using an averaging technique that takes into account all the transformations that align each subject to the current reference geometry. The update to the current reference geometry is given by

$$I^{n+1}_{\text{mean}}(\mathrm{x}^h) = \frac{1}{N}\sum_{i=1}^{N} I_i\left(T^n_i \circ [T^n_{\text{mean}}]^{-1}(\mathrm{x}^h)\right), \tag{4}$$

where N is number of images in the data set, x^h is the original grid, I_i are the anatomical MR images, $i = 1, 2, \ldots, N$, T^n_i is the mapping that registers the ith subject to the nth reference geometry, and T^n_{mean} is the average of the transformations T^n_i at the nth iteration defined as $T^n_{\text{mean}} = \frac{1}{N}\sum_{i=1}^{N} T^n_i$. The term $[T^n_{\text{mean}}]^{-1}$ is the inverse of the average of the transformations T^n_{mean}, and $\circ$ denotes the composition of transformations.

Repeating the update process in (4) leads to an average geometry I_{mean} and a collection of transformations aligning the anatomical MR images to I_{mean}. We can then use these transformations to transform the diffusion tensors of all the diffusion-weighted MR images in the data set.

In our implementations, we assumed that the transformation T and displacement d obtained when aligning a template image to a reference image are related by the equation $T(\mathrm{x}^h) = \mathrm{x}^h + d(\mathrm{x}^h)$. An inverse for the transformation T may be approximated by

$$\begin{aligned}\left[T(\mathrm{x}^h)\right]^{-1} &\approx \mathrm{x}^h - d(\mathrm{x}^h)\\ &= \mathrm{x}^h - \left(T(\mathrm{x}^h) - \mathrm{x}^h\right)\\ &= -T(\mathrm{x}^h) + 2\mathrm{x}^h.\end{aligned}$$

Thus, an approximation of the inverse for the average transformation field T^n_{mean} is

$$\left[T^n_{\text{mean}}(\mathrm{x}^h)\right]^{-1} \approx -T^n_{\text{mean}}(\mathrm{x}^h) + 2\mathrm{x}^h. \tag{5}$$

An outline of the groupwise registration framework is given in Algorithm 1.

Algorithm 1. The Groupwise Registration Framework

1. Initialize $n = 0$.
2. Set an arbitrary image in the data set as the initial reference image I^n_{mean}.
3. Use multilevel non-parametric registration to register each image in the data set to I^n_{mean} and store the resulting transformation field T^n_i that aligns each pair of images.
4. Compute the average transformation field T^n_{mean} at the nth step.
5. Approximate the inverse of T^n_{mean} using the formula in (5).
6. Transform each image in the data set by interpolating the intensity values of each subject I_i over the composition $T^n_i \circ [T^n_{\text{mean}}]^{-1}(\mathrm{x}^h)$.
7. Compute the average of transformed images to obtain the new current reference geometry $I^{n+1}_{\text{mean}}(\mathrm{x}^h)$.
8. Update $n \leftarrow n + 1$.
9. Repeat steps 3 to 8 until the method converges.

4 Results

In this section, we present some of the results obtained after implementing the algorithm discussed in the previous section on a small database of three healthy porcine hearts. We will also comment on the efficiency of the pairwise registration method used to align the full hearts to the reference geometries and on how fast the groupwise registration algorithm converges to a stable average geometry.

The unweighted center axial slices of the 3D MR images of the three healthy pig hearts used in our experiments are displayed in Fig. 2(a)–(c). Figure 2(d) shows the subjects superimposed on each other. Observe how varied the subjects are in terms of their heights and radii. Note that the image relating to Fig. 2(b) was set as the initial reference geometry, i.e., I^0_{mean}.

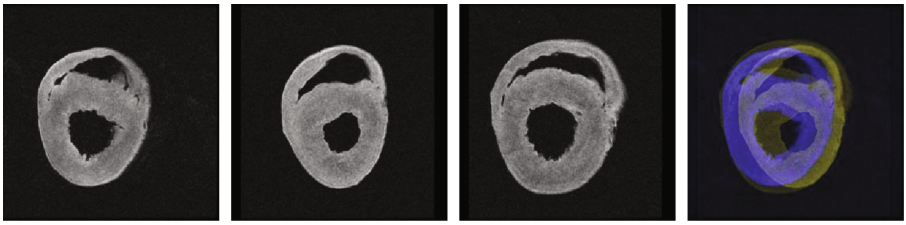

Fig. 2. Variability of heart geometries. (a)–(c) The three anatomical MR images used in our data set and (d) the three hearts overlaid onto each other.

We now observe the efficiency of the pairwise registration method implemented in our experiments. Shown in Fig. 3(a) and (e) are the initial and fourth reference geometries, respectively. The hearts in green masks in Fig. 3(b)–(d) and (f)–(h) are the transformed versions of the three subjects, superimposed against I^0_{mean} and I^4_{mean}, respectively. The pairwise registration algorithm that we used was able to determine reasonable transformations registering the full hearts to the current reference geometries, as demonstrated by the overlap between the template and reference images.

We observed that the method needs only a few iterations until it converges to a reasonable and stable average geometry. In our experiments, a stable average geometry was achieved after 5 to 7 iterations. Presented in Fig. 4 are the absolute changes $|I^n_{\text{mean}} - I^{n-1}_{\text{mean}}|$ in the reference geometries for iterations $n = 1, 2, 3, 4$. Figure 4 (c)–(d) being "almost black" indicates that there is minimal update made to the previous reference geometry. We also calculated the average change in the intensity values of the $256 \times 256 \times 128$ array $|I^n_{\text{mean}} - I^{n-1}_{\text{Imean}}|$ for the first seven iterations. The average change in intensity values dropped from more approximately 0.055 to 0.010, where the intensity change was is in the interval $[0, 1]$. The results are displayed in Fig. 5.

In Fig. 6, we show the first reference geometry and the computed average geometry and compared how the reference geometry changed after 7 iterations.

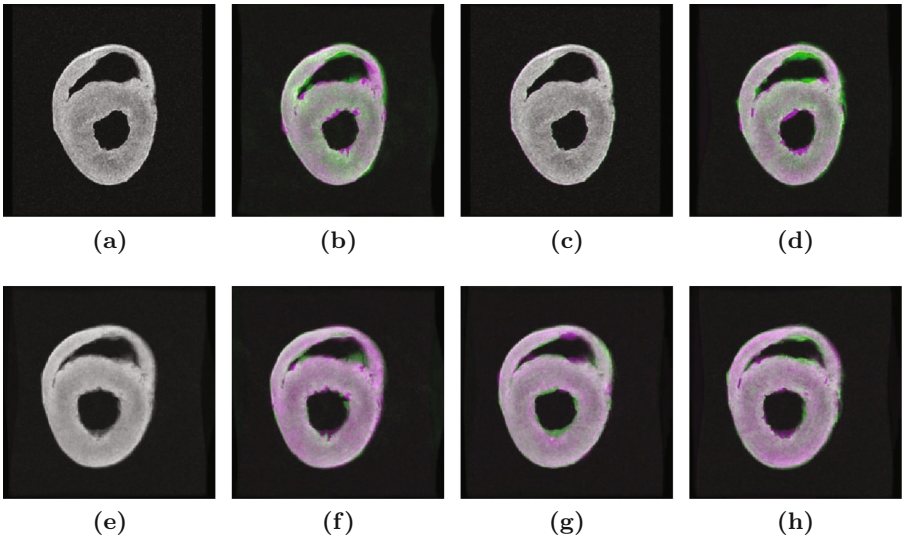

Fig. 3. Efficiency of the Pairwise Registration. (a) Initial reference geometry, (b)–(d) [in green mask] Transformed versions of the hearts in Fig. 2 vs I^0_{mean} [in pink mask], (e) Fourth reference geometry, (f)–(h) [in green mask] Transformed versions of the subjects vs I^4_{mean} [in pink mask] (Color figure online)

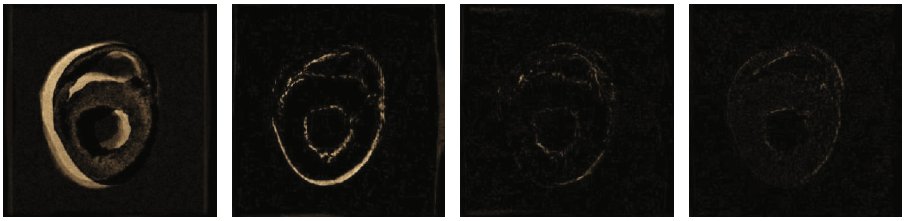

(a) $|I^1_{\text{mean}} - I^0_{\text{mean}}|$ **(b)** $|I^2_{\text{mean}} - I^1_{\text{mean}}|$ **(c)** $|I^3_{\text{mean}} - I^2_{\text{mean}}|$ **(d)** $|I^4_{\text{mean}} - I^3_{\text{mean}}|$

Fig. 4. Illustration of the rate of convergence of the groupwise framework to a stable reference geometry. (Color figure online)

Visually, the groupwise registration framework was able to normalize the heights and radii of the three subjects and converged to a reasonable average geometry.

Finally, we added an extra fourth subject to our data set, which significantly increased the variability of the cardiac geometries used in the above experiments. The additional subject is shown in Fig. 7(a), and again in Fig. 7(b) superimposed against the initial reference geometry. In Fig. 7(c), we present the result after aligning the aforementioned subject to the first reference image (Fig. 3(a)). Despite the differences in the cardiac features and geometries between I^0_{mean} and the new heart, the algorithm was still able to find a reasonable transformation that registers the two images. Groupwise registration converged to a stable and

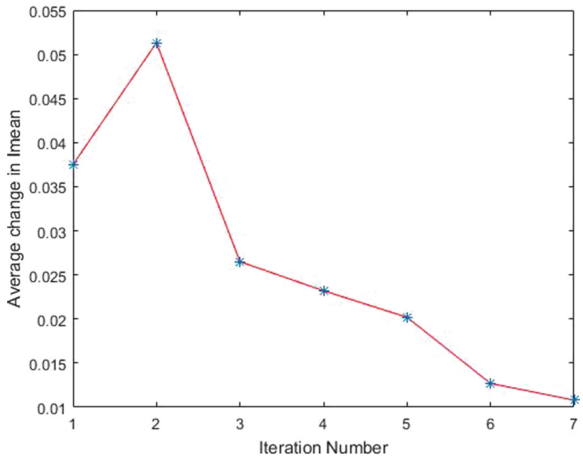

Fig. 5. Average change in I^n_{mean} after each iteration.

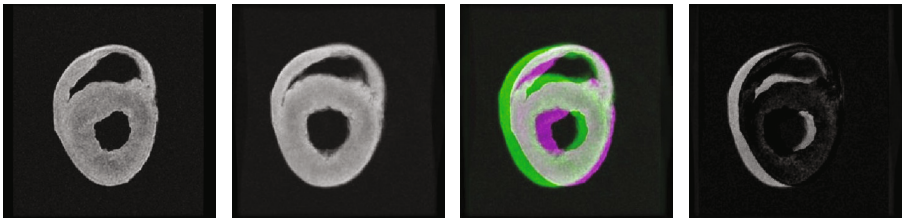

(a) I^0_{mean} **(b)** I^7_{mean} **(c)** I^0_{mean} vs I^7_{mean} **(d)** $|I^7_{\text{mean}} - I^0_{\text{mean}}|$

Fig. 6. Evolution of the reference geometries. (a) The initial reference geometry, (b) final average geometry, (c) final reference geometry overlaid onto the initial average geometry, and (d) the absolute change in the reference geometries.

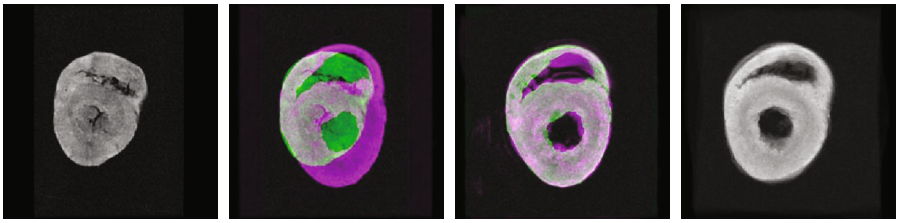

(a) **(b)** **(c)** **(d)**

Fig. 7. Introduction of an Additional Cardiac Data. The same framework was implemented with an outlier cardiac data ($N = 4$). (a) The newly added cardiac MR image, (b) New subject vs I^0_{mean}, (c) Result of the pairwise registration of (a) to I^0_{mean}, and (d) The average geometry computed from the database of the 4 porcine hearts.

reasonable average geometry after 9 iterations. The iterations were stopped when the absolute change in successive reference geometries was less than 0.01, i.e., $|I^n_{\text{mean}} - I^{n-1}_{\text{mean}}| < 0.01$.

5 Future Work and Conclusions

In this paper, we laid the foundation of a framework for building a statistical atlas for healthy porcine hearts by computing an average cardiac geometry from a small database of four freshly explanted healthy porcine hearts. We also demonstrated that the groupwise registration framework that we used converges to a stable average geometry. In addition, the multilevel non-parametric-based registration algorithm was able to successfully normalize the heart geometries and find reasonable transformations registering the subjects to each current reference geometry.

The next step would be to include more hearts in our experiments so that the average geometry would be a more accurate representation of a healthy porcine heart. Along with this, we are planning to compare the efficiency of the Diffeomorphic Log-Demons registration algorithm in [7] with the one we have implemented in this paper.

After building an average geometry, we aim to transform the diffusion tensors of the diffusion-weighted images of the anatomical MRIs to better understand porcine cardiac fiber and laminar sheet orientations needed in building a statistical atlas. The diffusion tensors can be transformed with the same deformations obtained in the pairwise registration step.

References

1. World Health Organization: Cardiovascular Diseases (2017)
2. Peyrat, J.M., Sermesant, M., Pennec, X., et al.: A computational framework for the statistical analysis of cardiac diffusion tensors: application to a small database of canine hearts. IEEE Trans. Med. Imag. **26**, 1500–14 (2007)
3. Lombaert, H., Peyrat, J.M., Croisille, P., et al.: Human atlas of the cardiac fiber architecture: study on a healthy population. IEEE Trans. Med. Imag. **31**(7), 1436–47 (2012)
4. Avants, B., Gee, J.C.: Shape averaging with diffeomorphic flows for atlas creation. In: 2nd IEEE International Symposium on Biomedical Imaging, vol. 1, 595–598 (2004)
5. Pop, M., Ghugre, N.R., Ramanan, V., et al.: Quantification of fibrosis in infarcted swine hearts by ex vivo late gadolinium-enhancement and diffusion-weighted MRI methods. Phys. Med. Biol. **58**(15), 5009–28 (2013)
6. Beg, M.F., Helm, P.A., McVeigh, E., Miller, M.I., Winslow, R.L.: Computational cardiac anatomy Using MRI. Magn. Reson. Med. Off. J. Soc. Magn. Reson. Med./ Soc. Magn. Reson. Med. **52**(5), 1167–1174 (2004)
7. Vercauteren, T., Pennec, X., Perchant, A., Ayache, N.: Symmetric log-domain diffeomorphic registration: a demons-based approach. In: Metaxas, D., Axel, L., Fichtinger, G., Székely, G. (eds.) MICCAI 2008, Part I. LNCS, vol. 5241, pp. 754–761. Springer, Heidelberg (2008). https://doi.org/10.1007/978-3-540-85988-8_90

8. Helm, P.: A Novel Technique for Quantifying Variability of Cardiac Anatomy: Application to the Dyssynchronous Failing Heart. Johns Hopkins University, Baltimore (2005)
9. Modersitzki, J.: Numerical Methods for Image Registration. Oxford University Press, Oxford (2004)
10. Modersitzki, J.: FAIR: Flexible Algorithms for Image Registration. SIAM, Philadelphia (2009)
11. Nocedal, J., Wright, S.J.: Numerical Optimization, 2nd edn. Springer, New York (2006)